Towards Molecular Understanding of the pH Dependence Characterizing NhaA of Which Structural Fold is Shared by Other Transporters

R. Mondal [1], A. Rimon [1], G. Masrati [3], N. Ben-Tal [3], A. Friedler [2] and E. Padan [1]*

*1 - **Department of Biological Chemistry,** The Alexander Silberman Institute of Life Sciences, The Hebrew University of Jerusalem, Edmond J. Safra Campus, Givat Ram, Jerusalem 91904, Israel*
*2 - **Institute of Chemistry,** The Hebrew University of Jerusalem, Edmond J. Safra Campus, Givat Ram, Jerusalem 91904, Israel*
*3 - **Department of Biochemistry and Molecular Biology,** George S. Wise Faculty of Life Sciences, Tel-Aviv University, Ramat-Aviv, 69978 Tel-Aviv, Israel*

***Correspondence to E. Padan:** etana.padan@mail.huji.ac.il (E. Padan)*
https://doi.org/10.1016/j.jmb.2021.167156
Edited by Nieng Yan

Abstract

Na^+/H^+ antiporters comprise a super-family (CPA) of membrane proteins that are found in all kingdoms of life and are essential in cellular homeostasis of pH, Na^+ and volume. Their activity is strictly dependent on pH, a property that underpins their role in pH homeostasis. While several human homologues have long been drug targets, NhaA of *Escherichia coli* has become the paradigm for this class of secondary active transporters as NhaA crystal structure provided insight into the architecture of this molecular machine. However, the mechanism of the strict pH dependence of NhaA is missing. Here, as a follow up of a recent evolutionary analysis that identified a 'CPA motif', we rationally designed three *E. coli* NhaA mutants: D133S, I134T, and the double mutant D133S-I134T. Exploring growth phenotype, transport activity and Li^+-binding of the mutants, we revealed that Asp133 does not participate directly in proton binding, nor does it directly dictate the pH-dependent transport of NhaA. Strikingly, the variant I134T lost some of the pH control, and the D133S-II134T double mutant retained Li^+ binding in a pH independent fashion. Concurrent to loss of pH control, these mutants bound Li^+ more strongly than the WT. Both positions are in close vicinity to the ion-binding site of the antiporter, attributing the results to electrostatic interaction between these residues and Asp164 of the ion-binding site. This is consistent with pH sensing resulting from direct coupling between cation binding and deprotonation in Asp164, which applies also to other CPA antiporters that are involved in human diseases.

Introduction

NhaA, of the large and diverse cation/proton antiporters (CPA) superfamily, is the main sodium/proton antiporter in *Escherichia coli*, exchanging $2H^+$ per $1Na^+$. It has homologues in enterobacteria, including many pathogens.[1] Several human CPAs (distant homologues of NhaA) are potential drug targets because their malfunction was associated with essential hypertension,[2] diabetes[3] and cancer.[1,4,5] Furthermore, Na^+/H^+ antiporters are critical for salt resistance in plants, an important issue in view of the spread of arid soils.[6]

NhaA is most extensively studied, and its crystal structure has been determined,[7] followed by the structural determination of its homo- and heterologues.[8,9] NhaA is a homodimer,[8,10–12] and its momomeric structure[7] (Fig. 1) has provided key structural insights into the function and regulation of this class of antiporters. It opened the way to structure-based interdisciplinary studies that other-

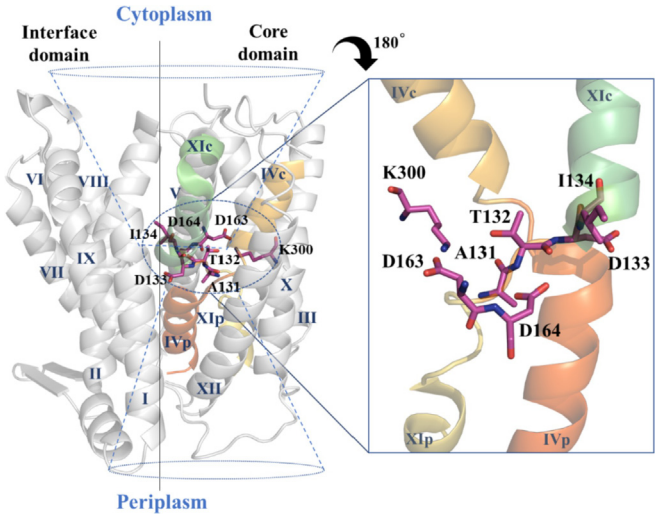

Figure 1. The crystal structure of the NhaA monomer (PDB.ID: 4ATV) and the relevant amino acid residues around Asp163 and Asp164, the putative cation biding site. Trans membrane segments (TMs) are denoted with Roman numerals, and c or p stands for cytoplasmic side or periplasmic side, respectively. The cytoplasmic funnel and the periplasmic funnel are represented as dotted line. The frame to the right displays a close-up view of the NhaA fold signature, two antiparallel inverted TMs IV and XI which are interrupted in their middle by extended chains crossing each other. The residues predicted to change ion specificity and cation binding are shown in stick representation using PyMOL software.

wise could not have been carried out. The crystal structure of NhaA monomer was determined at pH 4 as a down regulated monomer,[7] and then at pH 3.5 in its dimeric form.[8] The NhaA monomer, which is fully functional,[13] is comprised of 12 transmembrane (TM) helices, packed in two domains (Figure 1): an interface domain, which connects the two NhaA monomers; and a core domain. Between the two domains, two discontinues funnels open leading to the ion binding site, which is accessible from either the cytoplasm or periplasm in what is known as an alternating access mechanism.[14]

The NhaA structural fold is unique[15] and increasing number of secondary transporters share this fold in prokaryotes[9,16–19] and recently in eukaryotes.[20] In spite of the large diversity within the NhaA-fold, TMs III–V and X–XII invariantly share topologically inverted repeats.[7] Furthermore, TMs IV and XI are unwound in their middle and the respective extended chains cross each other in the middle of the membrane to form the X-shaped hallmark of the NhaA fold (Figure 1).

The Na^+ binding site has not been resolved in any of the crystal structures of the NhaA homologues.[16,18,19,21] Nevertheless, indirect structural and functional data predict that NhaA cation-binding site includes Asp163 and Asp164, the most evolutionarily conserved and irreplaceable residues[22,23] (Figures 1 and 2).

As a secondary transporter, NhaA harnesses the downhill movement of protons across the plasma membrane to facilitate the uphill antiport of Na^+ or Li^+ against their electrochemical gradient.[24,25] NhaA mediates an electrogenic transport with a stoichiometry of two protons that enter the cell per one cation that exits.[24,25] Thus, it renders the bacterial cell resistance to lithium/sodium toxicity even at alkaline pH.[26–28] NhaA has a very high turnover rate and is drastically dependent on pH,[25,29] NhaA is inactive below pH 6.5, and its activity increases upon pH elevation, reaching the maximal value at pH 8.5.

NhaA shares similar drastic pH dependence with most other prokaryotic and eukaryotic Na^+/H^+ antiporters because this characteristic underpins their role in pH homeostasis. Thus, NhaA mutants, which lost pH regulated activity, concurrently lost their capacity to render the cells resistant to alkaline pH.[26,30] Cells lacking NhaA are sensitive to alkaline pH.[28] In Eukaryotes, NHE1 is responsible for pH homeostasis both in cells and organelles.[31] Importantly, the pH dependence of this antiporter determines the set point for the cell pH homeostasis (for review see[26]) However, the molecular mechanism of the antiport pH regulation has remained elusive and many questions regarding the pH response of NhaA remained open. For example, does the drastic pH dependence of NhaA simply reflect competition between H^+ and Na^+/Li^+ on the same active site? Or, does pH affect another rate-limiting step of the transport cycle? In molecular terms: which are the residues in the NhaA proton pathway? Which residue's p*K*a is essential for the pH regulation? What is the role of the residues around it in maintaining the critical p*K*a?

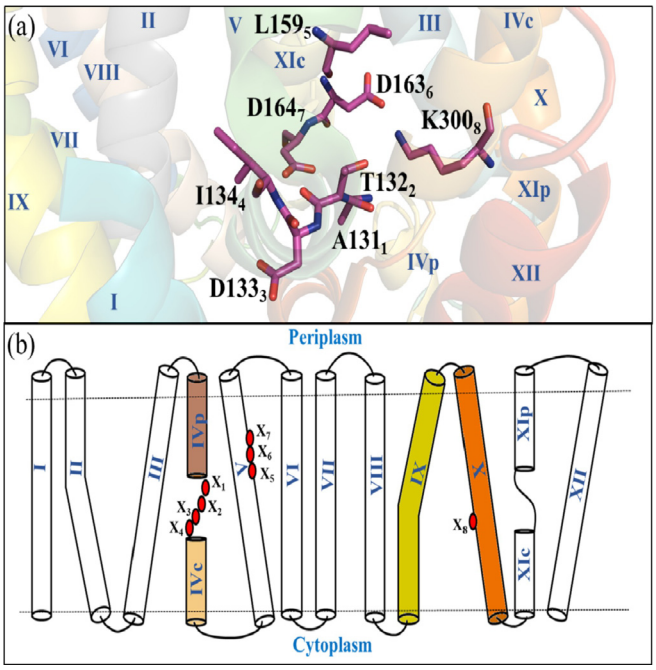

Figure 2. The CPA motif. (a) A close-up view of the structure of the eight residues forming the CPA motif in stick representation. Their corresponding position in the motif is indicated in subscript. (b) Two-dimensional representation of the NhaA structure with the CPA motif. The twelve transmembrane segments are designated in Roman numbers. The membrane boundaries are shown as dashed line. The eight motif residues are represented in red ovals (denoted as X_1, X_2, X_3,. . . . . X_8).

A step forward towards answering these questions has recently been made by the comprehensive evolutionary analysis of more than 6,500 different CPAs that sampled the vast sequential diversity of this superfamily.[32] This study revealed an evolutionarily conserved motif (CPA-motif) of eight amino acids clustered around the NhaA putative active site in the core domain of the protein (Figure 2). This motif appears to determine the characteristics of the antiport determinants.

Here, we focus on positions 1-through-4 of the CPA-motif, which includes the unwound section of TM-IV in NhaA including Ala131$_1$, Thr132$_2$, Asp133$_3$ and Ile134$_4$ (the numbers in the subscript correspond to the position in the CPA-motif; Figures 1 and 2). Structural data suggests that position two of the CPA motif participates in ion coordination through its backbone.[18]. However, the exact role of the first, third and fourth positions is still debated. Specifically, the first position of the CPA motif was suggested to confer potassium selectivity in some CPA1 members.[32] As such, it is less relevant for the function of NhaA, a CPA2 member, which is highly specific to Na^+ and Li^+.[33] Asp133$_3$, position three of the motif, was suggested to mediate the following four structural/functional roles: i) Compensation of the N-termini partial positive dipoles of TMs IVc and XIp (Figure 1).[7] Indeed, the negative charge of Asp133 was found critical for the stability of the NhaA fold.[34,35] ii) Participation in the transport activity, as its replacements greatly affect the apparent K_m of the antiporter.[34–36] iii) Facilitation of the transport of one out of the two protons transported by NhaA under certain conditions.[37] iv) Participation in the mechanism of the pH dependence of NhaA[34,35]; The functionality of Ile134$_4$, at the fourth position of the CPA-motif, has not yet been explored. In light of the above, we designed three mutants D133S and I134T, and the double mutant D133S-I134T, based on the distribution of amino acids found in the third and fourth positions of the CPA-motif.[32] Exploring growth phenotype, transport activity and Li^+-binding of the mutants, revealed unprecedented results providing important novel insights into the molecular mechanism of the strict pH regulation of NhaA and homologous antiporters important in health and disease.

Results

To explore the roles of the amino acid residues in the unwound section of NhaA- TM IV (position 3 and 4 of the CPA-motif, Figures 1 and 2), we followed the recent evolutionary analysis[32] and constructed three mutants, D133S and I134T, and the double mutant D133S-I134T (DM) in WT NhaA and in Cys-less NhaA. The evolutionary analysis showed that in other CPA members, such as Kef-like antiporters (K^+ selective antiporters[38,39]) and the

electrogenic NapA transporter (an NhaA homologue),[16] this aspartate is often replaced by serine. We therefore asked what would be the effect of replacing Asp133 with serine on the various suggested roles of Asp133 in NhaA.

Position four of the CPA-motif shows strong preference for hydrophobic amino acids, for example, in NhaA it is populated by isoleucine ($Ile134_4$). However, Kef-like antiporters are an exception, where position four feature the polar residue threonine. These transporters have some unique characteristics, while most CPAs transport sodium, Kef-like antiporters are selective to potassium[38] and, under certain conditions they have been suggested to mediate a channel-like potassium efflux. Thus, we asked whether Thr replacement of Ile134 or the double mutant, D133S-I134T, would change the NhaA cation-selectivity.

Plasmids bearing the NhaA mutations, were transformed into EP432 cells. This strain, lacking the Na^+/H^+ antiporters genes *nha*A and *nha*B, cannot grow on high Na^+/Li^+ selective media (0.6 M NaCl at pH 7 or pH 8.3, and 0.1 M LiCL at pH 7) unless transformed with a plasmid pAXH3 bearing WT NhaA (positive control).[27] EP432 cells transformed with the empty vector, pBR322, served as a negative control (Figure 3).

The NhaA-variants proteins expressed very well in membranes vesicles isolated from the respective strains amounting to 45–85% of the WT (Figure S1). Notably, because all variants were expressed from multi-copy plasmids, their expression, even the lowest, was far above the level expressed from a single chromosomal gene that confers a sodium resistant phenotype.[30]

All NhaA variants grew on a non-selective LBK media (Figure 3). The WT and the single mutant D133S also grew on all selective plates (0.6 M NaCl or 0.1 M LiCl at pH 7, and 0.6 M NaCl at pH 8.3). Mutant I134T grew only on the selective plates at pH 7 but did not grow in 0.6 M NaCl at pH 8.3. The DM mutant bearing strain could not grow on any of the selective agar plate. All Cys-Less NhaA variants behaved like NhaA variants.

The antiporter activity was determined in isolated inverted membrane vesicles of the respective strains at different pH values (Figure 4). The WT showed the characteristic pH dependent Na^+/H^+ antiporter activity. Namely, not active below pH 6.5 and increased activity up to a maximum between pH 7.5 and pH 8.5[25,29] (Figure 4). The

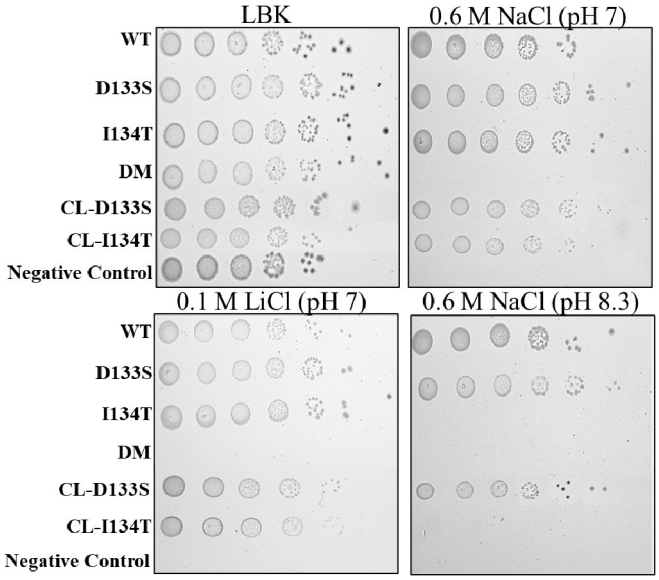

Figure 3. Growth phenotype of mutants, D133S, I134T, and D133S-I134T (DM). *E. coli* strain EP432, carrying inactivated *nha*A and *nha*B genes, was transformed with plasmid pAXH3 bearing WT NhaA (positive control) or NhaA mutants D133S, I134T, DM (the double mutant D133S-I134T), or pBR322, an empty vector, as negative control. Growth resistance to Na^+/Li^+ was performed as described in Methods section. Cells grown in modified L broth (LBK, with NaCl replaced by KCl) (OD_{600nm} 0.5) were tested for growth resistance to Li^+ and Na^+ at different pH-values as indicated. The positive control EP432/pAXH3 (first line) expressing WT NhaA grows under all conditions. The negative control EP432/pBR322 (last line) grows only on non-selective agar plates (LBK). Lines 2–4, mutants constructed in pAXH3; The D133S mutant grows similar to the WT but in slightly smaller colonies. I134T grows similar to the WT at 0.1 M LiCl or 0.6 M NaCl at pH 7 but cannot grow at alkaline pH (0.6 M NaCl, pH 8.3). The cells of DM grow only on non-selective conditions (LBK) but fails to grow on any of the selective media. Lines 5 and 6, the growth pattern of mutants constructed in pCL-AXH3 and marked CL. The experiments were conducted for three times with identical results. The standard deviation was 3–5%.

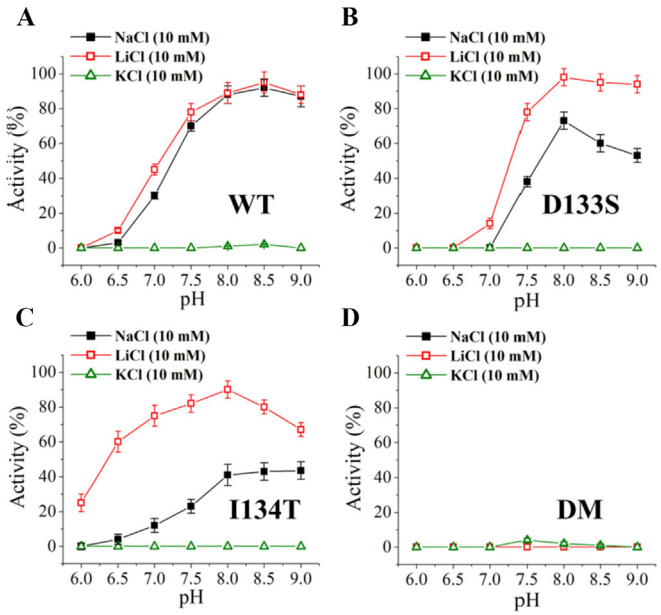

Figure 4. The pH dependence of the antiporter activity in isolated everted membrane vesicles of WT and the mutants D133S, I134T and DM. Everted membrane vesicles were prepared from EP432 cells expressing the indicated NhaA variants. The antiporter activity were determined at the indicated pH values using acridine orange fluorescence to monitor ΔpH. Fluorescence quenching occurs upon addition of D-lactate due to activation of respiration causing an influx of protons into the vesicles. Fluorescence de-quenching caused by the addition of 10 mM NaCl/LiCl/KCl indicates proton influx by NhaA activity upon addition of the respective ions. The antiporter activity expressed in percentage of dequenching is shown versus external pH. All experiments were repeated at least three times and the error bars represent standard deviation.

single mutant D133S showed Na^+/H^+ activity that is slightly lower than the WT (Figure 4) with 5 fold higher apparent K_m for Na^+ (2.7 mM) and 10 fold higher apparent K_m for Li^+ (0.2 mM) and pH-dependency similar to the WT (Figure 4). Membranes isolated from cells of the single mutant I134T showed even lower activity but with similar pH dependence (Figure 4). In marked contrast, membranes isolated from the DM mutant were inactive at all pH values both with Na^+ as well as with Li^+ similar to the negative control. None of the mutant strains showed K^+/H^+ antiport (Figure 4).

Inactivation of transport can result from interruptions to any step in the transport cycle. This includes ligand binding, conformational changes that lead to transport, energy coupling, and unfolding of the protein etc. It was therefore most interesting to test whether the affinity purified proteins of the double mutant and the single-mutants are stable and exhibit ligand binding nonetheless. We purified the variant proteins and validated that they are stable and not harmed, by testing their temperature sensitivity, as expressed in CD spectra (Figure 5). The results show that the DM is as stable as the WT; both have similar T_m around 74 °C. The single mutants are slightly less stable; Their T_m is around 64 °C. Although, as-yet we do not have the atomic structure of the mutants, their protein stability excludes dramatic changes in their native structure.

To measure Li^+ binding by the purified proteins of the variants, as a function of pH, we used Isothermal Titration Calorimetry (ITC) (Figures 6, 7 and Tables 1). As observed previously,[40] the WT protein bound Li^+ in a pH dependent fashion (Figure 6), very similar to the NhaA transport activity (Figure 4).[25,29] Maximum binding is at pH 8.5. Binding decreases at pH 8 and completely decays at pH 7.5 and below (Figure 6). Surprisingly, and in marked contrast to the WT, the DM, which did not exhibit any antiporter activity (Figure 4), nevertheless binds Li^+ in a pH independent fashion between pH 7 to 9 (Figure 6). Furthermore, the K_d of Li^+ binding of the DM is around 0.3 mM throughout pH values 7.5–9 (Table 1). This is 4 times lower than the 1.3 mM K_d of the WT (Table 1) at pH 8.5, and more than 10-fold lower at pH 8.

Similar to the WT, the variant D133S retains the pH dependence of binding Li^+; no binding up to pH 8 (not shown) and maximal binding at pH 8.5 (Figure 7). In marked contrast to variant D133S and the WT, the Li^+ binding of the I134T variant was pH independent between pH 7.5-pH 9 and only at pH 7 and below its Li^+ binding decreased. Notably, the I134T mutant seems to retain much of its pH-dependent sodium binding (Figure 4(C)).

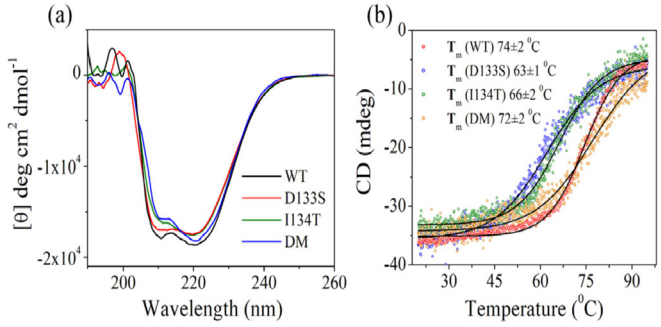

Figure 5. CD spectra of WT and the mutants D133S, I134T and DM. (a) The proteins were affinity-purified and re-suspended in dialysis buffer titrated to pH 8.5 by using Tris base. The far-UV CD spectra was taken for each protein (~4 μM) at 4 °C (b) The thermal unfolding transition midpoint (T_m) values of the WT NhaA and the mutants, were determined from the corresponding inflection points by typical ellipticity curves at 222 nm as a function of temperature. Traces are representative from three different measurements.

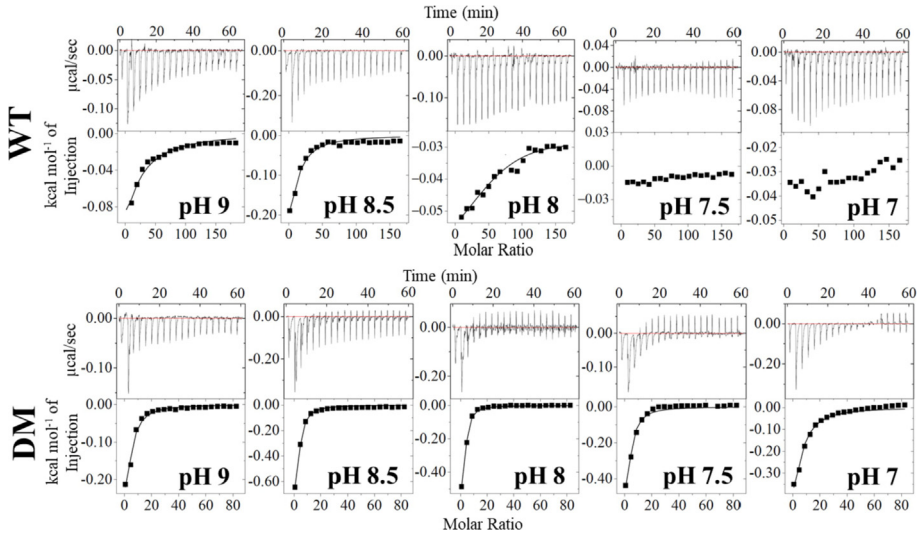

Figure 6. The pH dependence of Li^+ binding to WT and the DM (D133S-I134T) proteins determined by ITC. Top panels: Heat liberated when 40/20 mM LiCl solution is injected into the experimental chamber containing ~ 50 μM WT/DM protein at 10 °C in reaction buffer (containing 50 mM BTP, 150 mM choline chloride, 5 mM $MgCl_2$, 10% sucrose, 0.015% DDM and the pH adjusted by using HCl). Bottom panels: The area underneath each deflection is integrated and represents the total heat exchanged (squares). The black lines are the best fits to a single-site binding isotherm. Averaged thermodynamic parameters are reported in Table 1 for WT and DM, respectively. All ITC experiments are repeated at least three times and the errors are calculated accordingly in the Table 1.

Again, as observed with the double mutant, the K_d of the I134T mutant was lower than that of mutant D133S and the WT (Table 1). Hence, compared to WT NhaA, the mutation I134T decreased the pH dependence of Li^+ binding, and the DM mutant completely lost pH dependence. Furthermore, in parallel to the decrease in pH dependence of variants I134T and the DM, their Li^+ affinity increased, decreasing significantly their Li^+ binding K_d as compared to the WT and D133S mutant.

Discussion

The comprehensive evolutionary analysis of the CPA superfamily[32] has recently discovered the CPA-motif (Figure 2) which suggested that residues Ala131, Thr132, Asp133 and Ile134 in the unwound portion of TM IV of the NhaA fold (Figure 1) may be involved in ion selectivity and pH regulation of NhaA. To examine the functional/structural roles of the latter two residues we constructed the mutants D133S, I134T and the respective DM (D133S-I134T).

The functional/structural roles of Asp133 in NhaA

The essential structural role of Asp133 for NhaA-fold stability is supported by its high evolutionary conservation across all CPAs (electrogenic and

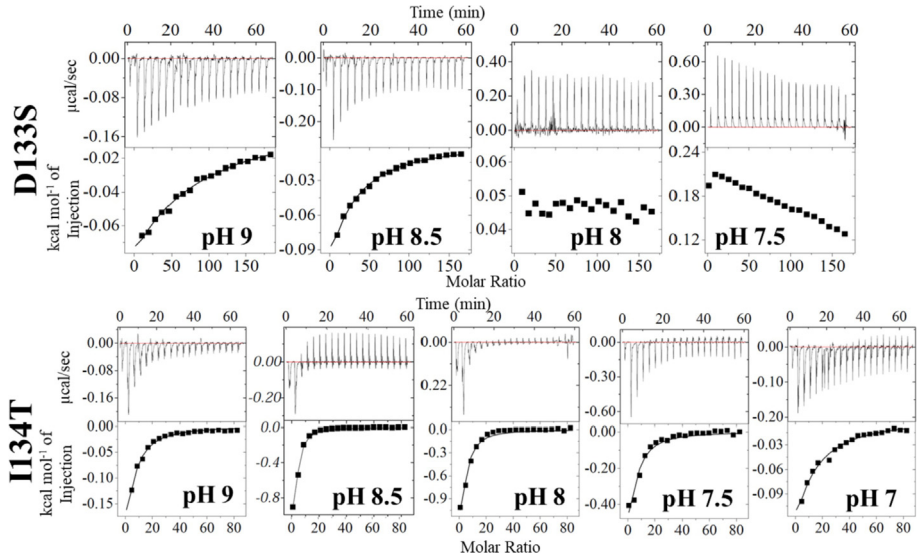

Figure 7. The pH dependence of Li^+ binding to the D133S and I134T mutants' proteins determined by ITC. Top panels: Heat liberated when 40/20 mM LiCl solution is injected into the experimental chamber containing ~50 µM D133S/I134T affinity purified proteins at 10 °C in buffer described in Figure 5. Bottom panels: as described in Figure 5. All ITC experiments are repeated at least three times and the errors are calculated accordingly.

Table 1 Dissociation constant (K_d) values for Li^+ binding to the NhaA-WT and mutants in different pH values at 10 ℃.

pH	*WT* K_d (mM)	*D133S* K_d (mM)	*I134T* K_d (mM)	*DM* K_d (mM)
9	2.96 ± 0.04	10 ± 0.2	1.4 ± 0. 2	0.35 ± 0.04
8.5	1.30 ± 0.02	3.9 ± 0.1	0.05 ± 0.001	0.31 ± 0.03
8	4.55 ± 0.08	–	0.1 ± 0.01	0.28 ± 0.02
7.5	–	–	0.58 ± 0.02	0.27 ± 0.03
7	–	–	3.7 ± 0.1	0.59 ± 0.05

electroneutral),[32] and its location in the core of the protein, as observed in NhaA's crystal structure (Figure 1).[7] Its negative charge compensates the N-termini partial positive dipoles of TMs IVc and XIp (Figure 1),[7], structurally stabilizing NhaA.[34,35]

The electrogenicity of NhaA (exchanging one cation with two protons[24,25]) enables *E. coli* to grow in alkaline conditions as the influx of protons helps maintain constant cytoplasmic pH.[26] An electroneutral mutant of NhaA was unable to grow under such conditions.[32] As can be seen in Figure 3, the D133S mutant grows in selective media including alkaline medium, similar to the WT although with smaller colonies. Hence, this mutated antiporter is most likely still electrogenic. Consistently, *Thermus thermophilus* NapA, a homologous CPA antiporter that similar to NhaA facilitates electrogenic transport,[41] lacks an aspartate at position three of the CPA-motif. Instead, like our NhaA D133S mutant, NapA has a serine in this position. It follows that Asp133 is not one of the two primary proton donors in the WT-NhaA or else replacing it with a non-titratable residue, such as serine, would not allow the mutant to survive in alkaline pH. In this regard, supplementary mechanisms for electrogenicity have been suggested[37,42] in which Asp133 serves as a secondary proton carrier, only when the primary proton donors are impaired, but the physiological relevance of these mechanisms are debated.

Notably, D133S mutation increased 5 fold the apparent K_m for Na^+ (2.7 mM) and 10 fold for Li^+ (0.2 mM) with respect to the WT (0.5 and 0.02 mM, respectively) accounting for the slightly smaller colonies of D133S at alkaline pH (Figure 3). These results are consistent with previous results demonstrating that Asp133 is sensitive to mutations in a way that directly affects antiport activity.[22] Specifically, replacement of Asp133 with Cys[35,36] or Ala[34] greatly affects the apparent K_m of the antiporter to Na^+ and Li^+. This suggests that at least in some stages during the transport cycle, Asp133 interacts with the transported cations, and/or that it contributes to energy coupling, and/or participates in the conformational changes of NhaA.[34,35]

Being a titratable residue, Asp133 could theoretically be part of NhaA's "pH sensor" even if it is not the primary proton carrier. However, our results presented here show that it is highly unlikely. The D133S substitution had little effect on the pH-dependent activity of NhaA as can be seen in Figure 4 as compared to the WT. Accordingly, our ITC results show that D133S binds Li^+ in a pH dependent fashion similar to the WT (Figure 7). Indeed, to "sense" pH in serine substitution (D133S) the serine must undergo

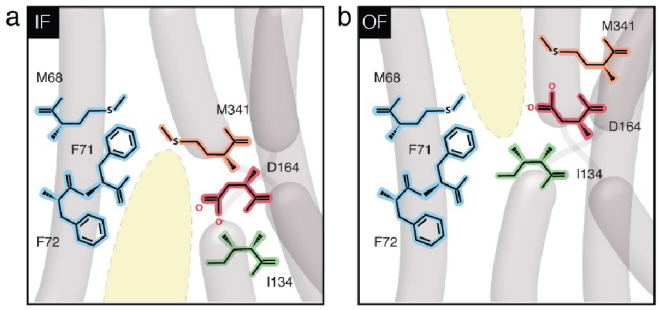

Figure 8. Proposed outward (OF) and inward (IF) conformations of NhaA highlighting the role of IL134. Schematic 2-dimensional projections of NhaA's core in IF (7) (a) and OF [43] (b) conformations, showing the important residues around the binding site Asp164. The two discontinuous funnels leading to the antiporter's binding site, denoted by D164, are shown colored yellow. As NhaA adopts an IF conformation, the hydrophobic interactions between F71, F72 and M68 on TM-2 and M341 on TM-11 form the upper cap of the cytoplasmic funnel, and D164 is accessible from the cytoplasm. As the antiporter adopts an OF state, F71, F72 and M68 interact with I134 on TM-4 to form the base of the periplasmic funnel, and D164 is accessible from the periplasm [43].

deprotonation, which is highly unlikely in view of its very high pKa value in solution (~13).

To conclude, our results show that Asp133 is not the primary proton carrier in NhaA, nor is it part of the antiporter's pH-sensing mechanism, but it could be involved in the reaction cycle of the antiporter by contributing to the cation coordination. Indeed, previously we had demonstrated that the main chain of Asp133 participates in cation binding.[35]

The functional/structural roles of Ile134 in NhaA

We recently predicted what could be the unknown long sought outward-facing conformation of NhaA, suggesting a critical structural role of Ile134 in the conformational dynamics of NhaA.[43] As shown in the crystal structure,[7] when NhaA is in its inward facing conformation, the hydrophobic interactions between Phe71, Phe72 and Met68 on TM-II and M341 on TM-XI form the lower cap of the cytoplasmic funnel (Figure 8a). Conversely, in the (predicted) outward facing conformation Phe71, Phe72 and Met68 interact with Ile134 on TM-IV to form the base of the periplasmic funnel (Figure 8b). Our results, strongly support this suggestion as Thr-replacement of Ile134 (I134T) compromised growth on selective medium at alkaline pH (Figure 3) and markedly inhibited antiporter activity (Figure 4).

The D133S-I134T DM and the single mutant I134T impair the pH dependence of NhaA while increasing its affinity to Li^+

The DM did not grow on any selective media, while the I134T mutant grew only at pH 7 (Figure 3). The DM was inactive (Figure 4), and less than 40% activity remained in the I134T mutant as compared to WT. Our ITC measurements show that surprisingly, both mutants nevertheless bind Li^+, albeit with impaired pH dependence. Li^+ binding by the I134T mutant significantly drops below pH 7 (Figure 7) while the drop in Li^+ binding of the WT (Figure 6) and D133S mutant (Figure 7) is at higher pH of below 8. Strikingly, the DM binds Li^+ independently of pH in the 7 to 9 range (Figure 6). Furthermore, the Li^+ binding affinity of mutants I134T and D133S-I134T increased concurrent to the loss of pH dependence (Table 1). Hence, it is likely that the cumulative effect of both the I134T and the D133S mutations affect the pH dependence of Li^+ binding to NhaA.

How do the II134T and D133S-II134T mutations change the pH dependence of Li^+ binding? Having ruled out the possibility that D133 directly senses the pH (see above and Figures 3 and 4), we are left with the possibility that the mutations change the p*K*a of a nearby amino acid residue that is involved in proton/Li^+ binding. According to the crystal structures,[8] evolutionary conservation[32] and experimental results,[22,23] Asp163 is an essential residue of the binding site, is charge paired with Lys300 and located remotely from both Asp133 and Ile134 (Figure 1). Therefore, mutations of Asp133 and Ile134 are less likely to affect it. On the other hand, Asp164, the other essential residue of the binding site,[7,8,22,23,32] is located in close proximity to both Asp133 and Ile134 (Figures 1 and 2(a)). It is thus plausible that mutations of the latter residues affect the p*K*a of Asp164. In the WT, the negative charge on both Asp133 and Asp164 would result in electrostatic repulsion, which is energetically unfavorable. To avoid that, the intrinsic p*K*a of one or both aspartates would most likely be higher than their p*K*a in solution. Indeed, recent fixed-charge[8] and the continuous constant pH molecular dynamics (CpHMD) studies[44] showed that the p*K*a of Asp164 is the highest (p*K*a 6.0) among the active-site aspartates, confirming its role as a proton binder/donor residue.[42] This high intrinsic p*K*a of WT-Asp164 is mechanistically advantageous in

that it would facilitate a fast and easy shift between the protonated and de-protonated forms upon transport at physiological conditions. We suggest that mutations I134T and DM lower the intrinsic p*K*a of Asp164 because of two effects. The first is the loss of electrostatically repulsive interactions between Asp164 and position 133, in which the aspartate was replaced with serine (mutant D133S). The second is the addition of a hydrogen bond between Asp164 and position 134 in which isoleucine was replaced with threonine (I134T). With its lower p*K*a in the DM, D164 would remain deprotonated, explaining the pH-independent Li^+-binding of the DM, as opposed to the wild type, and the stronger effect of the DM compared to the I134T mutant.

Lastly, the increased affinity of I134T and the DM mutants to Li^+ is most likely mainly due to the I134T substitution. Ile134 is close enough to the Li^+ binding site, Asp164 (Figures 1 and 2a), such that by mutating Ile134 to threonine, the polarity of the latter's oxygen atom can stabilize the Li^+ ion through favorable dipole-charge interaction. Asp133 is slightly more distant and therefore its effect is weaker. Still, it can interact with Li^+ through long-range ionic interactions, conferring further stabilization. When Asp133 is replaced with serine, which lacks a full charge, the weak stabilization effect is eliminated and the affinity decreases. However, replacement of Ile134, to I134T is sufficient to recover the affinity that was lost upon the replacement of D133 with serine.

Concluding remarks

Our experimental results contradict the recently emerging hypothesis that Asp133 acts as a primary/secondary proton carrier in NhaA.[37] Furthermore, it is not a pH-sensor, as its protonation states do not affect transport directly. However, a negative or polar charge in this position might contribute indirectly to the pH-dependent transport of NhaA via electrostatic interactions with Asp164. As the DM demonstrates, slight changes to the electrostatic environment surrounding Asp164 could result in a pH-independent ion binding. Taken together, our results support the straightforward pH-dependent transport mechanism whereby the cations compete with protons for the same binding site.[45] Calinescu et al.'s model was abstract, and here we attribute the cation-proton exchange, and resulting pH-dependence, to Asp164. Furthermore, we highlight the important role of the residues surrounding it in maintaining its p*K*a. Indeed, when the pH is lower than the intrinsic p*K*a of WT Asp164, the latter is constantly protonated and the antiporter is inactive. When pH rises above the intrinsic p*K*a of Asp164, it deprotonates and is able to bind cations. It is noteworthy, though, that this is not the complete story and the antiport cycle includes additional pH affected step(s). These data have wide ramifications for studies focusing on pH homeostasis in cells or the development of drugs that target Na^+/H^+ antiporters in humans.

Materials and Methods

Plasmids, bacterial strains, and culture conditions

pAXH3 is a plasmid expressing His-tagged NhaA.[13] pCl-AXH3 is a plasmid bearing Cys-Less NhaA.[46] EP432 is an *E. coli* K-12 derivative, which is *mel*BLid, *Δnha*A1::*kan*, *Δnha*B1::*cat*, *ΔlacZY*, *thr*1.[28] TA16 is an *E. Coli* K-12 derivative (*nhaA*+, *nhaB*+, *lacI*^{Q}) and is otherwise isogenic to EP432.[13,28]

Cells were grown either in Luria broth (LB) or in modified LB (LBK) in which NaCl was replaced with KCl. The medium was buffered with 60 mM 1,3-Bis[tris(hydroxymethyl)methylamino]propane (BTP). For plates, 1.5 % agar was used. To test cell resistance to Li^+ and Na^+, EP432 cells transformed with the respective plasmids were grown on LBK to A_{600} of 0.5. Samples (2 μl) of serial 10-fold dilutions of the cultures were spotted onto agar plates containing the selective media: modified LB in which NaCl was replaced with the indicated concentrations of NaCl or LiCl at the various pH levels and incubated for 2 days at 37 °C.

Site-directed mutagenesis

Site-directed mutagenesis was conducted following a polymerase chain reaction-based protocol[47] with either pAXH3 or pCL-AXH3 as templates. All plasmids carrying mutations are designated by the name of the mutation.

Affinity purification of NhaA variants

Over expression of the NhaA variants[46,48] and affinity purification (Ni-nitrilo triacetic acid-agarose; Qiagen) were performed as described previously.[40]

Detection and quantitation of NhaA and its mutated derivatives in the membrane

Total membrane protein was determined according to Bradford.[49] The expression level of His-tagged NhaA mutants was determined by resolving the Ni-NTA-purified proteins by SDS-PAGE, staining the gels with Coomassie Blue and quantifying the band densities by Image Gauge (Fuji) software.[46]

Isolation of everted membrane vesicles and assay of Na^+/H^+ antiport activity

EP432 cells transformed with the respective plasmids were grown in LBK medium, and everted membrane vesicles were prepared and used to determine the Na^+/H^+ antiport activity as described previously.[50,51] The assay of antiport activity was based upon the measurement of Na^+/

Li^+ induced changes in ΔpH as measured by acridine orange, a fluorescent probe of ΔpH. The fluorescence assay was performed with 2.5 ml of reaction mixture containing 50–100 μg of membrane protein, 0.5 μM acridine orange, 150 mM cholineCl, 50 mM BTP, and 5 mM $MgCl_2$, and the pH was titrated with HCl as indicated. The membranes were energized by addition of D-lactate (2 mM, pH7 titrated by KOH), quenching of the fluorescence was allowed to achieve a steady state, and then Na^+/Li^+ (10 mM) was added. A reversal of the fluorescence level (dequenching) indicates that protons are exiting the vesicles in antiport with Na^+/Li^+. As shown previously, the end level of dequenching is a good estimate of antiport-activity, and the concentration of the ion that gives half-maximal dequenching is a good estimate of the apparent *K*m for Na^+ (or Li^+) of the antiporter.[52,53]

Isothermal Titration Calorimetric analysis (ITC)

ITC experiments were performed as previously described[40] using the micro-calorimeter ITC200 (MicroCal, GE Healthcare). The reaction mixture (300 μl contained: 50 mM BTP, 150 mM choline chloride, 5 mM $MgCl_2$, 10 % sucrose (pH 8.5), 40–50 μM protein and 0.015 % DDM (β-dodecyl-D-maltoside). For titration, 20/40 mM LiCl (dissolved in the same reaction buffer) was loaded into the injection syringe. Before data collection, the system was equilibrated to 10 °C with the stirring speed set to 500 rpm. Notably, all the ITC experiments were done at 10C, because the WT and mutants NhaA are not stable and aggregate at 25C under the experimental conditions of constant stirring for the 3–4 hrs for each experiment. Therefore, it is not possible to measure the binding at 25C. Titration curves for binding Li^+ were initiated by injection of 0.8 μL followed by successive 2-μL injections of the ligand every 200 s. Injections of ligands into reaction buffer without protein or reaction buffer into reaction buffer were performed to determine background corrections. The integrated heats from each injection, normalized to the moles of ligand per injection, were fit to a single-site binding isotherm using ORIGIN 7 software. The integrated peak of the first injection was excluded from the fit due to the large errors in the first step. For further details, see Ref.[40]

Circular dichroism (CD) spectroscopy measurements

CD measurements were made on a JASCO J-810CD Spectro-polarimeter (JASCO, Inc., Japan), using the supplied Spectra Manager software. The respective proteins (3–4 μM) were prepared in a solution containing 100 mM choline chloride, 5 mM $MgCl_2$, 25 mM citric acid, 10% sucrose, and 0.015% DDM. The respective pH levels were obtained by titration with KOH for pH 4 and with1.8 M Tris base for the other pH values. Spectra data were collected at 0.1-nm intervals at 4 °C, using a Peltier-Controlled Sample Compartment, and variable temperature measurements were made between 4 °C and 95 °C at a wavelength of observed higher peak (near 222 nm) with 0.2 °C data interval. T_m was determined by plotting data in.

Author Contributions

G.M., E.P., N.B.-T and A.F. conceptualized the project. G.M. performed the phylogenetic analyses, evolutionary conservation analyses, and homology modeling; R.M and A.R. constructed the mutants and conducted the functional assays; E.P. A.F. G.M. and N.B.-T. wrote the manuscript with input from all authors. E.P. and A.F. thank the Israel Science Foundation (ISF, grant No. 284/12 and No. 939/14, respectively).

Acknowledgements

R.M. thanks Lady Davies fellowship of the Hebrew University 2019. This study was supported by a German-Israeli Project Cooperation (DIP) grant to NB-T and E.P. G.M. was funded in part by a fellowship from the Edmond J. Safra Center for Bioinformatics at Tel-Aviv University and the Madaim scholarship. N.B.-T.'s research is supported in part by the Abraham E. Kazan Chair 5 in Structural Biology, Tel Aviv University.

Declaration of Competing Interest

The authors declare that they have no known competing financial interests or personal relationships that could have appeared to influence the work reported in this paper.

Appendix A. Supplementary material

Supplementary data to this article can be found online at https://doi.org/10.1016/j.jmb.2021.167156.

Received 25 April 2021;
Accepted 8 July 2021;
Available online 14 July 2021

Keywords:
NhaA antiporter;
NhaA;
Cation-binding;
pH-dependent Cation binding

Abbreviations:
CPA, Cation/Proton Antiporters; TM, transmembrane; BTP, Bis[tris(hydroxymethyl)methylamino]propane; LB, Luria broth; Ni-NTA, Ni-nitrilo triacetic acid-agarose; DDM, β-dodecyl-D-maltoside; DM, double mutant

References

1. Padan, E., Landau, M., (2016). Sodium-proton (Na+/H+) antiporters: properties and roles in health and disease in The alkali metal ions: their role for life. Springer International, Cham, Switzerland.
2. Xiang, M., Feng, M., Muend, S., Rao, R., (2007). A human Na+/H+ antiporter sharing evolutionary origins with bacterial NhaA may be a candidate gene for essential hypertension. *PNAS*, **104** (47), 18677–18681.
3. Deisl, C. et al, (2013). Sodium/hydrogen exchanger NHA2 is critical for insulin secretion in beta-cells. *PNAS*, **110** (24), 10004–10009.
4. Ko, M., Quinones-Hinojosa, A., Rao, R., (2020). Emerging links between endosomal pH and cancer. *Cancer Metastasis Rev.*, **39** (2), 519–534.
5. Pedersen, S.F., Counillon, L., (2019). The SLC9A-C Mammalian Na(+)/H(+) Exchanger Family: Molecules, Mechanisms, and Physiology. *Physiol. Rev.*, **99** (4), 2015–2113.
6. Bassil, E., Blumwald, E., (2014). The ins and outs of intracellular ion homeostasis: NHX-type cation/H^+ transporters. *Curr. Opin. Plant Biol.*, **22**, 1–6.
7. Hunte, C. et al, (2005). Structure of a Na+/H+ antiporter and insights into mechanism of action and regulation by pH. *Nature*, **435** (7046), 1197–1202.
8. Lee, C. et al, (2014). Crystal structure of the sodium-proton antiporter NhaA dimer and new mechanistic insights. *J. Gen. Physiol.*, **144** (6), 529–544.
9. Shi, Y., (2013). Common folds and transport mechanisms of secondary active transporters. *Annu. Rev. Biophys.*, **42**, 51–72.
10. wGerchman, Y., Rimon, A., Venturi, M., Padan, E., (2001). Oligomerization of NhaA, the Na+/H+ antiporter of Escherichia coli in the membrane and its functional and structural consequences. *Biochemistry*, **40** (11), 3403–3412.
11. Hilger, D., Polyhach, Y., Padan, E., Jung, H., Jeschke, G., (2007). High-resolution structure of a Na+/H+ antiporter dimer obtained by pulsed electron paramagnetic resonance distance measurements. *Biophys. J.*, **93** (10), 3675–3683.
12. Williams, K.A., Geldmacher-Kaufer, U., Padan, E., Schuldiner, S., Kuhlbrandt, W., (1999). Projection structure of NhaA, a secondary transporter from Escherichia coli, at 4.0 A resolution. *EMBO J.*, **18** (13), 3558–3563.
13. Rimon, A., Tzubery, T., Padan, E., (2007). Monomers of the NhaA Na+/H+ antiporter of Escherichia coli are fully functional yet dimers are beneficial under extreme stress conditions at alkaline pH in the presence of Na+ or Li+. *J. Biol. Chem.*, **282** (37), 26810–26821.
14. Jardetzky, O., (1966). Simple allosteric model for membrane pumps. *Nature*, **211** (5052), 969–970.
15. Padan, E., Michel, H., (2015). NhaA, a unique structural fold of secondary active transporters. *Israel J. Chem.*, **55**, 1233–1239.
16. Lee, C. et al, (2013). A two-domain elevator mechanism for sodium/proton antiport. *Nature*, **501** (7468), 573–577.
17. Hu, N.J., Iwata, S., Cameron, A.D., Drew, D., (2011). Crystal structure of a bacterial homologue of the bile acid sodium symporter ASBT. *Nature*, **478** (7369), 408–411.
18. Wohlert, D., Kuhlbrandt, W., Yildiz, O., (2014). Structure and substrate ion binding in the sodium/proton antiporter PaNhaP. *eLife*, **3**, e03579.
19. Wohlert, D., Grotzinger, M.J., Kuhlbrandt, W., Yildiz, O., (2015). Mechanism of Na(+)-dependent citrate transport from the structure of an asymmetrical CitS dimer. *eLife*, **4**, e09375.
20. Winkelmann, I. et al, (2020). Structure and elevator mechanism of the mammalian sodium/proton exchanger NHE9. *EMBO J.*,, e105908.
21. Paulino, C., Wohlert, D., Kapotova, E., Yildiz, O., Kuhlbrandt, W., (2014). Structure and transport mechanism of the sodium/proton antiporter MjNhaP1. *eLife*, **3**, e03583.
22. Inoue, H., Noumi, T., Tsuchiya, T., Kanazawa, H., (1995). Essential aspartic acid residues, Asp-133, Asp-163 and Asp-164, in the transmembrane helices of a Na+/H+ antiporter (NhaA) from Escherichia coli. *FEBS Letters*, **363** (3), 264–268.
23. Galili, L., Herz, K., Dym, O., Padan, E., (2004). Unraveling functional and structural interactions between transmembrane domains IV and XI of NhaA Na+/H+ antiporter of Escherichia coli. *J. Biol. Chem.*, **279** (22), 23104–23113.
24. Taglicht, D., Padan, E., Schuldiner, S., (1993). Proton-sodium stoichiometry of NhaA, an electrogenic antiporter from Escherichia coli. *J. Biol. Chem.*, **268** (8), 5382–5387.
25. Dwivedi, M., Sukenik, S., Friedler, A., Padan, E., (2016). The Ec-NhaA antiporter switches from antagonistic to synergistic antiport upon a single point mutation. *Sci. Rep.*, **6**, 23339.
26. Krulwich, T.A., Sachs, G., Padan, E., (2011). Molecular aspects of bacterial pH sensing and homeostasis. *Nat. Rev. Microbiol.*, **9** (5), 330–343.
27. Padan, E., Bibi, E., Ito, M., Krulwich, T.A., (2005). Alkaline pH homeostasis in bacteria: new insights. *BBA*, **1717** (2), 67–88.
28. Pinner, E., Kotler, Y., Padan, E., Schuldiner, S., (1993). Physiological role of nhaB, a specific Na+/H+ antiporter in Escherichia coli. *J. Biol. Chem.*, **268** (3), 1729–1734.
29. Taglicht, D., Padan, E., Schuldiner, S., (1991). Overproduction and purification of a functional Na+/H+ antiporter coded by nhaA (ant) from Escherichia coli. *J. Biol. Chem.*, **266** (17), 11289–11294.
30. Rimon, A., Gerchman, Y., Kariv, Z., Padan, E., (1998). A point mutation (G338S) and its suppressor mutations affect both the pH response of the NhaA-Na+/H+ antiporter as well as the growth phenotype of Escherichia coli. *J. Biol. Chem.*, **273** (41), 26470–26476.
31. Orlowski, J., Grinstein, S., (2007). Emerging roles of alkali cation/proton exchangers in organellar homeostasis. *Curr. Opin. Cell Biol.*, **19** (4), 483–492.

32. Masrati, G. et al, (2018). Broad phylogenetic analysis of cation/proton antiporters reveals transport determinants. *Nature Commun.*, **9** (1), 4205.
33. Zuber, D. et al, (2005). Kinetics of charge translocation in the passive downhill uptake mode of the Na+/H+ antiporter NhaA of Escherichia coli. *BBA*, **1709** (3), 240–250.
34. Rimon, A., Dwivedi, M., Friedler, A., Padan, E., (2018). Asp133 Residue in NhaA Na(+)/H(+) Antiporter Is Required for Stability Cation Binding and Transport. *J. Mol. Biol.*, **430** (6), 867–880.
35. Rimon, A., Kozachkov-Magrisso, L., Padan, E., (2012). The unwound portion dividing helix IV of NhaA undergoes a conformational change at physiological pH and lines the cation passage. *Biochemistry*, **51** (47), 9560–9569.
36. Galili, L., Rothman, A., Kozachkov, L., Rimon, A., Padan, E., (2002). Trans membrane domain IV is involved in ion transport activity and pH regulation of the NhaA-Na(+)/H(+) antiporter of Escherichia coli. *Biochemistry*, **41** (2), 609–617.
37. Patino-Ruiz, M. et al, (2019). Replacement of Lys-300 with a glutamine in the NhaA Na(+)/H(+) antiporter of Escherichia coli yields a functional electrogenic transporter. *J. Biol. Chem.*, **294** (1), 246–256.
38. Fujisawa, M., Ito, M., Krulwich, T.A., (2007). Three two-component transporters with channel-like properties have monovalent cation/proton antiport activity. *PNAS*, **104** (33), 13289–13294.
39. Fujisawa, M., Wada, Y., Ito, M., (2004). Modulation of the K^+ efflux activity of Bacillus subtilis YhaU by YhaT and the C-terminal region of YhaS. *FEMS Microbiol. Lett.*, **231**, 211–217.
40. Maes, M., Rimon, A., Kozachkov-Magrisso, L., Friedler, A., Padan, E., (2012). Revealing the ligand binding site of NhaA Na+/H+ antiporter and its pH dependence. *J. Biol. Chem.*, **287** (45), 38150–38157.
41. Uzdavinys, P. et al, (2017). Dissecting the proton transport pathway in electrogenic Na(+)/H(+) antiporters. *PNAS*, **114** (7), E1101–E1110.
42. Henderson, J.A., Huang, Y., Beckstein, O., Shen, J., (2020). Alternative proton-binding site and long-distance coupling in Escherichia coli sodium-proton antiporter NhaA. *PNAS*, **117** (41), 25517–25522.
43. Masrati, G., Mondal, R., Rimon, A., Kessel, A., Padan, E., Lindahl, E., Ben-Tal, Nir, (2020). An angular motion of a conserved four-helix bundle facilitates alternating acess transport in TtNapA and NhaA. *Proc. Nat. Acad Sci.*,.
44. Huang, Y., Chen, W., Dotson, D.L., Beckstein, O., Shen, J., (2016). Mechanism of pH-dependent activation of the sodium-proton antiporter NhaA. *Nature Commun.*, **7**, 12940.
45. Calinescu, O., Paulino, C., Kuhlbrandt, W., Fendler, K., (2014). Keeping it simple, transport mechanism and pH regulation in Na+/H+ exchangers. *J. Biol. Chem.*, **289** (19), 13168–13176.
46. Olami, Y., Rimon, A., Gerchman, Y., Rothman, A., Padan, E., (1997). Histidine 225, a residue of the NhaA-Na+/H+ antiporter of Escherichia coli is exposed and faces the cell exterior. *J. Biol. Chem.*, **272** (3), 1761–1768.
47. Ho, S.N., Hunt, H.D., Horton, R.M., Pullen, J.K., Pease, L. R., (1989). Site-directed mutagenesis by overlap extension using the polymerase chain reaction. *Gene*, **77** (1), 51–59.
48. Gerchman, Y., Rimon, A., Padan, E., (1999). A pH-dependent conformational change of NhaA Na(+)/H(+) antiporter of Escherichia coli involves loop VIII-IX, plays a role in the pH response of the protein, and is maintained by the pure protein in dodecyl maltoside. *J. Biol. Chem.*, **274** (35), 24617–24624.
49. Bradford, M.M., (1976). A rapid and sensitive method for the quantitation of microgram quantities of protein utilizing the principle of protein-dye binding. *Anal. Biochem.*, **72**, 248–254.
50. Goldberg, E.B. et al, (1987). Characterization of a Na+/H+ antiporter gene of Escherichia coli. *PNAS*, **84** (9), 2615–2619.
51. Rosen, B.P., (1986). Ion extrusion systems in Escherichia coli. *Methods Enzymol.*, **125**, 328–336.
52. Schuldiner, S., Fishkes, H., (1978). Sodium-proton antiport in isolated membrane vesicles of Escherichia coli. *Biochemistry*, **17** (4), 706–711.
53. Tsuboi, Y., Inoue, H., Nakamura, N., Kanazawa, H., (2003). Identification of membrane domains of the Na+/H + antiporter (NhaA) protein from Helicobacter pylori required for ion transport and pH sensing. *J. Biol. Chem.*, **278** (24), 21467–21473.